Original Article

Diagnostic value of combined magnetic resonance imaging techniques in the evaluation of Parkinson disease

Qing Cao[1#], Xiaowei Han[2#], Dongping Tang[3], Hao Qian[4], Kun Yan[4], Xun Shi[5], Yaowei Li[1*], Jiangong Zhang[5*]

[1]Department of Radiology, Guangzhou Xinhai Hospital, Guangzhou, China; [2]Department of Radiology, The Affiliated Drum Tower Hospital of Nanjing University Medical School, Nanjing, China; [3]Department of Science and Education, Guangzhou Xinhai Hospital, Guangzhou, China; [4]Department of Neurology, Guangzhou Xinhai Hospital, Guangzhou, China; [5]Department of Nuclear Medicine, The First People's Hospital of Yancheng, The Fourth Affiliated Hospital of Nantong University, Yancheng, China

Contributions: (I) Conception and design: Q Cao, X Han; (II) Administrative support: D Tang, Y Li; (III) Provision of study materials or patients: H Qian, K Yan, D Tang; (IV) Collection and assembly of data: Q Cao, Y Li, H Qian, K Yan; (V) Data analysis and interpretation: Q Cao, Y Li, X Shi, X Han, J Zhang; (VI) Manuscript writing: All authors; (VII) Final approval of manuscript: All authors.

[#]These authors contributed equally to this work and should be considered as co-first authors.

[*]These authors contributed equally for the senior authorship.

Correspondence to: Jiangong Zhang, MD. Department of Nuclear Medicine, The First People's Hospital of Yancheng, The Fourth Affiliated Hospital of Nantong University, No. 66, Renmin South Road, Yancheng 224006, China. Email: jiangongzh@126.com; Yaowei Li, MD. Department of Radiology, Guangzhou Xinhai Hospital, No. 167, Xingang West Road, Haizhu District, Guangzhou 510300, China. Email: weiweihao168@sina.com.

Background: The incidence of Parkinson disease (PD) has been increasing each year. The development of new magnetic resonance imaging (MRI) technology can help understand its pathogenesis and identify more effective imaging-based biological indicators.

Methods: The clinical and MRI imaging data of 40 patients with PD and 40 healthy controls were analyzed. All participants underwent susceptibility-weighted imaging (SWI), neuromelanin-sensitive magnetic resonance imaging (NM-MRI), and T2*mapping sequence examination. The diagnostic value of single and combined multiparameter indicators was analyzed using the receiver operating characteristic curve.

Results: Compared with the healthy control group, the PD group showed significant differences in the disappearance of bilateral "swallow tail sign", the distribution volume of melanocytes in the substantia nigra and the smaller volume in the bilateral substantia nigra, the maximum signal of the locus coeruleus and the smaller and average volume in the bilateral substantia nigra, and the values of T2* and R2* in the bilateral substantia nigra ($P<0.01$). The maximum and smaller value and the average value of the bilateral locus coeruleus signal were negatively correlated with the disease course duration ($P<0.05$), and the smaller distribution volume of the melanin neurons in the bilateral substantia nigra was negatively correlated with Hoehn and Yahr (H-Y) grade ($P<0.05$). In the joint diagnosis with multiple indicators, some composite parameters were found to be negatively correlated with H-Y grading ($P<0.05$), while others were negatively correlated with disease course duration ($P<0.05$). Joint use of multiple parameter indicators greatly improved diagnostic efficacy [area under the curve (AUC) =0.958].

Conclusions: The distribution volume of melanin in substantia nigra and the maximum value of locus coeruleus signal may be the biological imaging indicators for the early diagnosis, severity, and follow-up evaluation of PD. Compared with a single indicator, composite indicators used in combination with multiple techniques have a significantly better diagnostic efficacy for PD.

Keywords: Parkinson disease (PD); susceptibility-weighted imaging (SWI); neuromelanin-sensitive magnetic resonance imaging (NM-MRI); receiver operating characteristic curve; diagnostic efficacy

Submitted Jan 20, 2023. Accepted for publication Aug 08, 2023. Published online Aug 18, 2023.
doi: 10.21037/qims-23-87
View this article at: https://dx.doi.org/10.21037/qims-23-87

Introduction

Parkinson disease (PD) is a common degenerative disorder of the nervous system in which clinical symptoms worsen with an increase in the degree of neuronal degeneration (1). In China, the incidence rate of PD has continuously increased with the aging of the population, and the number of patients with PD in China is projected to reach 5 million by 2030 (2), which will place a heavy burden on both families and society. Recently, magnetic resonance imaging (MRI) has rapidly improved and shown considerable advantages in detecting nervous system diseases; thus, it is currently widely used in clinical settings (3). However, the value of using conventional MRI sequences or single-sequence images for PD diagnosis is limited. Consequently, there is an urgent need to develop the use of special imaging sequences and composite indicators in combination with multiple techniques to improve the detection and diagnostic efficacy in PD treatment.

The major neuropathological changes of PD include damage to substantia nigra neurons and the related disorder of dopamine receptor passage; the substantia nigra is located on the ventral side of the dorsal tegmental region of the mesencephalon, on the outer side of the red nucleus, and on the dorsal side of the crus cerebri. It is a gray-matter band adjacent to the crus cerebri, containing cell clusters of melanin, which are rich in dopamine. The increase of abnormal glial protein iron complex in the substantia nigra region induces the accumulation of neuroglia cell, leading to neuronal damage and expedited cell death (3,4). Susceptibility-weighted imaging (SWI) can more sensitively monitor the iron deposition area and its range. A normal substantia nigra shows a "swallow tail sign" change on SWI due to the decreased signal in nigrosome 1 during abnormal iron deposition. Importantly, SWI indirectly reflects the degeneration of dopamine-secreting neurons (5,6).

For other imaging modalities, neuromelanin-sensitive magnetic resonance imaging (NM-MRI) has been used to better display the distribution area of neuromelanin in the substantia nigra, locus coeruleus, and other regions. A decreased signal in the corresponding regions indirectly reflects the degeneration of melanin neurons (7). The T2*mapping sequence adopts the method of multiple echo acquisition within a gradient echo and obtains the R2* value through matrix operation to reflect the R2* weight. Because iron deposition shortens T2* and increases R2*, T2*mapping can be used to quantify iron deposition and monitor the development of PD (8). Previous studies have examined the use of a single sequence for PD detection and evaluation (9,10). However, manual sketching of the anatomical area of the substantia nigra to measure its signal or volume can easily lead to evaluation deviation due to the degeneration and unclear boundaries of neural tissue in the substantia nigra. In addition, the small volume of the locus coeruleus often leads to measurement errors and affects the accuracy of the analysis. Therefore, to improve the diagnostic accuracy in PD, it is necessary to further advance the measurement and evaluation methods of related PD indicators through the combination of MRI techniques (11-13).

This study aimed to explore the application of combining multiple MRI techniques in PD diagnosis, evaluate the correlation of combined MRI technique-related indicators with clinical stage and disease course, and evaluate the diagnostic value of the application of composite indicators used in combination with multiple techniques in PD. To this end, the high signal intensity area of NM-MRI distribution was delineated, the volume was measured, and the maximum value of the locus coeruleus signal was used for evaluation. SWI, NM-MRI, and T2*mapping were evaluated as composite indicators, and further correlation analysis with clinical scale scores were conducted. In addition, the sensitivity and specificity of each single index, as well as those of composite indicators, were analyzed. We present this article in accordance with the STROBE reporting checklist (available at https://qims.amegroups.com/article/view/10.21037/qims-23-87/rc).

Table 1 Parameter value of each sequence scan

Sequence	TR (ms)	TE (ms)	Voxel size (mm^3)	Number of slices	Slice spacing (mm)	Flip angle	Average times	Interpolation	IR (ms)
T2WI_TRA	5,103	119.9	0.67×0.60×5.00	23	1	150	2	–	–
T1WI_TRA	2,267	10.2	0.69×0.63×5.00	23	1	135	1	–	920
FLAIR_TRA	8,000	118.6	0.95×0.76×5.00	23	1	120	2	–	2,500
DWI_TRA	2,087	107.1	1.44×1.44×5.00	23	1	–	–	–	–
T2WI_SAG	5,683	121.8	0.77×0.65×5.00	23	1	145	1.2	–	–
FLAIR_COR	8,000	112.9	0.90×0.72×5.00	25	1	150	1.5	–	2,500
SWI_TRA	30.3	20	0.51×0.51×2.00	56	–	–	1	2	–
NM-MRI_TRA	738	10.54	0.62×0.44×3.00	22	0	130	5	–	–
T2*mapping_TRA	436.7	6.71/15.65/24.6/33.54/42.48	0.48×0.48×3.00	11	0.3	–	1	–	–

TR, repetition time; TE, time to echo; IR, inversion-recovery time; T2WI, T2-weighted imaging; TRA, transverse; T1WI, T1-weighted imaging; FLAIR, fluid-attenuated inversion recovery; DWI, diffusion-weighted imaging; SAG, sagittal; COR, coronal; SWI, susceptibility-weighted imaging; NM-MRI, neuromelanin-sensitive magnetic resonance imaging.

Methods

Study design and participants

This study recruited 40 patients with PD from the Department of Neurology of Guangzhou Xinhai Hospital from March 2020 to August 2022. The selection criteria were as follows: (I) PD diagnosis evaluated based on the patient's symptoms of motor delay, static tremor, or myotonia and meeting the Chinese diagnostic criteria for PD diagnosis (2020 version); (II) no contraindication of MRI and able to complete MRI examination; and (III) image quality meeting diagnostic criteria. The exclusion criteria were are as follows: (I) secondary Parkinson syndrome, such as organic psychosis of the nervous system or effects of medication; and (II) factors affecting image evaluation, such as traumatic brain injury, brain malformation development, and neurological- or psychiatric-related diseases. Data on patients' clinical medical history, Hoehn and Yahr (H-Y) scale grading, and multiparameter MRI results were collected.

Meanwhile, 40 healthy controls from employees or relatives of Guangzhou Xinhai Hospital were enrolled in the study. The inclusion criteria were as follows: (I) no motor or nonmotor symptoms associated with PD; (II) no family history of PD or essential tremor; (III) no contraindication to MRI and ability to undergo MRI examination; and (IV) image quality meeting diagnostic criteria. The exclusion criteria were as follows: (I) neurological and psychiatric disorders due to taking medication; and (II) traumatic brain injury, brain malformation development, or other factors that would influence image assessment.

This study was authorized by the ethics committee of Guangzhou Xinhai Hospital (No. GZXH-20200147) and was implemented on the basis of the principles of the Declaration of Helsinki (as revised in 2013). Written informed consent was obtained from all participants after detailed information concerning the research purpose, scanning duration, relevant risks, and examination considerations was provided.

Instruments and imaging methods

A 3.0 T magnetic resonance scanner (model No. uMR780; Union-Imaging Healthcare, Shanghai, China) with a 24-channel coil was used for head and neck scans. The routine MRI sequence consisted of the transverse axial [T1-weighted imaging (T1WI), T2WI, fluid-attenuated inversion recovery (FLAIR), diffusion-weighted imaging (DWI)], sagittal (T2WI), coronal (FLAIR), SWI, NM-MRI, and T2*mapping sequences. The NM-MRI sequence adopted united compressed sensing (uCS; fast factor 1.8) technology. All parameters are listed in *Table 1*. The total MRI scanning time was 28 minutes and 36 seconds.

Image preprocessing analysis

All collected image data were processed in a postprocessing workstation (model No. uWS-MR-R004; Union-Imaging Healthcare). Dr. Cao Q with 12 years of medical imaging

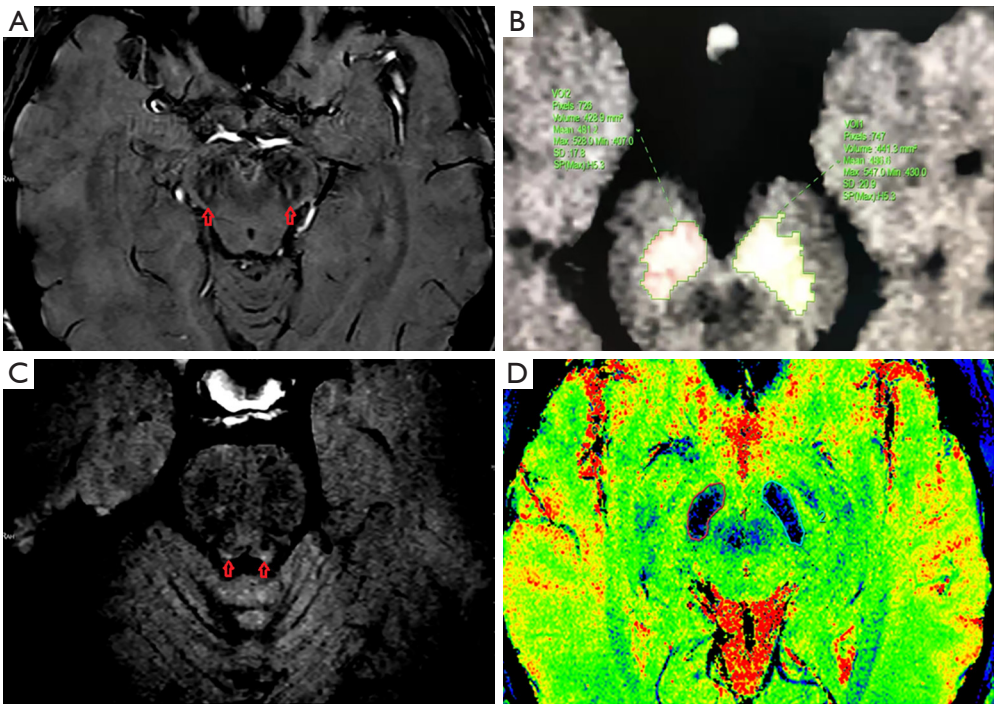

Figure 1 Display of the substantia nigra and locus coeruleus regions and corresponding indicator observations based on multiple MRI sequences. (A) Swallow tail sign displayed on SWI (the area is indicated by the red arrows). (B) The distribution of melanin in neurons of bilateral substantia nigra on NM-MRI (green outlined area). (C) The high signal intensity in bilateral locus coeruleus nuclei on NM-MRI (the red arrows indicate the high signal area). (D) The bilateral substantia nigra areas were outlined, and T2* and R2* values were obtained based on T2*mapping (dark blue area outlined by the wireframe). VOI, volume of interest; SD, standard deviation; SP, scale pixel; MRI, magnetic resonance imaging; SWI, susceptibility-weighted imaging; NM-MRI, neuromelanin-sensitive magnetic resonance imaging.

diagnosis experience, and Dr. Li Y, with 20 years of medical imaging diagnosis experience, evaluated the images, agreed on the principle of blindness, measured the relevant image indicators, and averaged the 2 measurements. The physicians evaluated the swallow tail sign based on the SWI chart and determined whether it had disappeared (*Figure 1A*) according to the following scoring scheme: 2 points, both sides of the swallow tail sign disappeared; 1 point, 1 side disappeared; and 0 point, no sign of disappearance of the swallow tail sign on either side. The layer-by-layer distribution of melanin in bilateral substantia nigra neurons on NM-MRI was recorded, and the volume and average signal value were calculated (*Figure 1B*).

Before images were collected, the appropriate window width and position were fixed to reduce visual and signal differences. We only delineated the high signal areas of the substantia nigra, without drawing the areas of attenuation. Images were collected without any gaps. The volume of high signal intensity areas in the distribution of melanin neurons was calculated layer by layer based on voxels, the volume of distribution of melanin in bilateral substantia nigra, and bilateral average value and smaller value; meanwhile, the measured signal was determined as the average value of the sketched area. Given that the locus coeruleus is small and the signal intensity of the locus coeruleus is higher than that of the surrounding tissues, the maximum signal value of its voxel level was first obtained by measuring the signals of the bilateral locus coeruleus areas. Then, the signals of the bilateral locus coeruleus areas were compared in each patient, and their smaller and average values were recorded (*Figure 1C*).

For T2*mapping data processing, some cases showed heavy skull-base magnetic susceptibility artifacts (3 cases in the PD group). In 4 cases in the PD group, multiple time to echo (TE) data points caused by skull-base plane motion could not be processed with motion correction, and thus these patients were not included. Ultimately, in 33 patients in the PD group and 40 patients in the healthy control

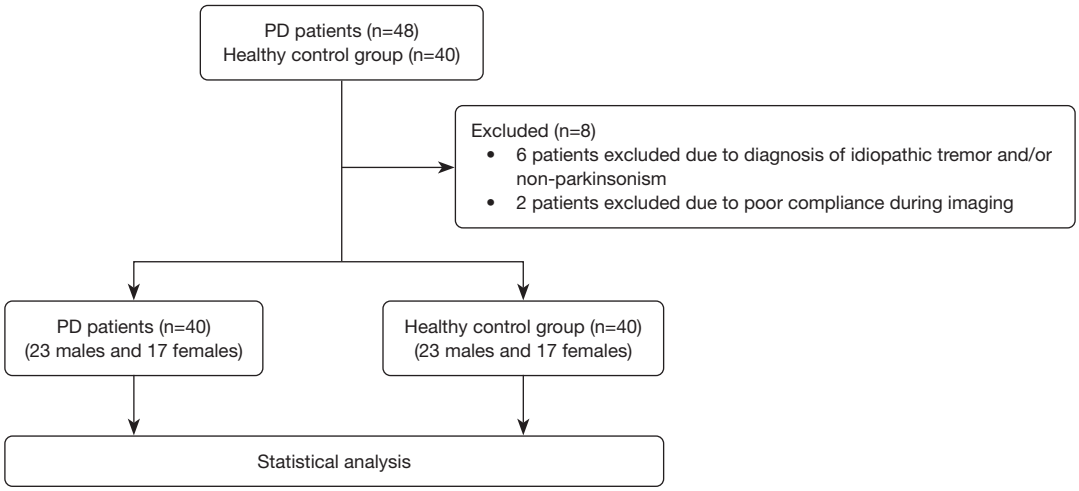

Figure 2 Diagram of study flow. PD, Parkinson disease.

group, bilateral substantia nigra areas were drawn while T2* and R2* values were calculated (*Figure 1D*) based on T2*mapping to quantitatively analyze iron deposition in the substantia nigra (14).

Statistical analysis

Kappa consistency test [disappearance of the SWI swallow tail sign: R_Kappa (right_weighted kappa coefficient) 0.822, P<0.001; L_Kappa (left_weighted kappa coefficient) 0.863, P<0.001] and intraclass correlation coefficient (ICC; all remaining measured values 0.6< ICC <1; P<0.001) consistency evaluation was used for the measurement values of the 2 doctors, with both doctors showing good consistency in their measurements. Between-group comparisons were performed using an independent samples *t*-test or chi-squared test. Pearson correlation analysis was used to evaluate the correlation between imaging indicators of each sequence and composite indicators used in combination with multiple techniques and clinical PD indicators. The area under the receiver operating characteristic curve (AUC) was used to analyze the threshold value of disappearance of the SWI swallow tail sign (SWI), distribution volume of NM-MRI melanin in the substantia nigra (NM-MRI_SN_volume), maximum signal value of locus coeruleus (NM-MRI_LCmax), and iron deposition in the T2*mapping R2* value in the substantia nigra area (T2*mapping_R2*) for the diagnosis of PD. In addition, the diagnostic value of the composite indicators used in combination with multiple techniques in PD was evaluated. Logistic regression analysis was conducted on each of the single and composite indicators, and the AUC of single and composite indicators were compared via the Delong test. All statistical analyses were performed using SPSS 22.0 (IBM Corp., Chicago, USA). A 2-tailed P value <0.05 was considered statistically significant.

Results

Patient characteristics

The MRIs of 48 patients were collected. However, 6 patients with idiopathic tremor did not meet the diagnostic criteria for PD, and 2 patients could not be evaluated due to poor image quality. Therefore, 40 patients (23 males and 17 females) were included in the PD group. The average patient age was 67.025±15.22 years, the average disease course duration was 6.51±6.06 years, and the average H-Y grade was 2.76±1.07. Meanwhile, the control group included 40 individuals (23 males and 17 females) with an average age of 62.150±12.35 years. There was no significant between-group difference in age (P=0.120), and the 2 groups were gender-matched (*Figure 2*).

Multiple technique image analysis

Between-group comparisons in the number of disappearances of bilateral swallow tail sign upon SWI evaluation

In the healthy control group, the swallow tail sign disappeared on the right and left in 2 (2/40) and in 3 (3/40)

Table 2 Intergroup comparison of bilateral swallow tail sign disappearance based on SWI

Indicator	Name	PD group (n=40), n (%)	Healthy control group (n=40), n (%)	χ^2	P value
R_swallow tail sign disappearance	Positive	31 (77.50)	2 (5.00)	43.378	<0.01
	Negative	9 (22.50)	38 (95.00)		
L_swallow tail sign disappearance	Positive	27 (67.50)	3 (7.50)	30.720	<0.01
	Negative	13 (32.50)	37 (92.50)		

Chi-squared test was used to compare the disappearance of bilateral swallow tail sign in SWI between the groups, with the difference being considered significant at a statistical threshold of P<0.05. The number outside the parentheses is the number of instances, and the number inside the parentheses bracket is the percentage within the group. SWI, susceptibility-weighted imaging; PD, Parkinson disease; R, right; L, left.

Table 3 Intergroup comparison of melanin signal in the substantia nigra and locus coeruleus based on NM-MRI

Indicator	PD group (n=40)	Healthy control group (n=40)	*t* value	P value
R_SN_volume of melanin	263.84±108.91	439.79±78.44	–8.291	<0.01
L_SN_volume of melanin	314.65±108.36	502.90±96.18	–8.218	<0.01
The small value of the bilateral SN_volume of melanin	252.73±98.98	435.87±76.44	–9.262	<0.01
Bilateral SN_volume average	289.25±103.05	471.35±82.56	–8.722	<0.01
R_LC_signal maximum	489.95±30.70	504.25±26.52	–2.229	0.029
L_LC_signal maximum	507.63±29.96	529.95±33.88	–3.122	0.003
The small value of the bilateral LC_ signal maximum	488.50±29.14	503.38±26.26	–2.398	0.019
Bilateral LC_ signal maximum average	498.79±28.72	517.10±28.60	–2.858	<0.01
R_SN_signal average	460.64±21.51	465.06±19.20	–0.970	0.335
L_SN_signal average	469.20±23.38	472.00±17.25	–0.610	0.544

Intergroup comparison of melanin signals in the substantia nigra and locus coeruleus according to the independent samples *t*-test, with the difference being considered significant at a statistical threshold of P<0.05. Data are presented as mean ± SD. NM-MRI, neuromelanin-sensitive magnetic resonance imaging; PD, Parkinson disease; SD, standard deviation; R, right; L, left; SN, substantia nigra; LC, locus coeruleus.

cases, respectively. In the PD group, the swallow tail sign disappeared on the right and left in 31 (31/40) and 27 cases (27/40), respectively. Statistical differences were found between the groups in terms of right swallow tail sign disappearance (χ^2=43.378; P<0.01) and left swallow tail sign disappearance (χ^2=30.720; P<0.01) (*Table 2*). There was also a statistical difference between the 2 groups in the disappearance scores of swallow tail sign (*t*=9.842; P<0.01).

Between-group comparison of melanin signal and distribution in the substantia nigra and locus coeruleus based on NM-MRI

There were significant differences between the control group and PD group with respect to the distribution volume of melanin in the bilateral substantia nigra (right: *t*=–8.291, P<0.01; left: *t*=–8.218, P<0.01), the smaller value of volume in the bilateral substantia nigra (*t*=–9.262; P<0.01), the average value of volume in the bilateral substantia nigra (*t*=–8.722; P<0.01), the maximum signal value of the bilateral locus coeruleus (right: *t*=–2.229, P=0.029; left: *t*=–3.122, P=0.003), the smaller value of the bilateral locus coeruleus (*t*=–2.398; P=0.019), and the average value of the bilateral locus coeruleus (*t*=–2.858; P<0.01). Meanwhile, no significant difference was observed in the mean signal values of the bilateral substantia nigra (right: *t*=–0.970, P=0.335; left: *t*=–0.610, P=0.544) (*Table 3*).

Table 4 Intergroup comparison of T2* and R2* values in the substantia nigra based on T2*mapping

Indicator	PD group (n=33)	Healthy control group (n=40)	*t* value	P value
R_SN_T2* value	29.31±2.15	31.59±2.11	−4.546	<0.01
R_SN_R2* value	35.45±2.39	32.70±2.06	5.285	<0.01
L_SN_T2* value	29.58±2.71	31.68±2.24	−3.621	<0.01
L_SN_R2* value	35.06±2.89	32.53±2.20	4.252	<0.01

Intergroup comparison of T2* and R2* values in the substantia nigra according to the independent samples *t*-test, with the difference being considered significant at a statistical threshold of P<0.05. Data are presented as mean ± SD. SD, standard deviation; PD, Parkinson disease; R, right; L, left; SN, substantia nigra.

Between-group comparison of T2* and R2* values in the substantia nigra based on T2*mapping

The control and PD groups showed significant differences in the T2* (right: t=−4.546, P<0.01; left: t=−3.621, P<0.01) and R2* values (right: t=5.285, P<0.01; left: t=4.252, P<0.01) of the bilateral substantia nigra (*Table 4*).

Correlation analysis of the PD group

Correlation analysis was conducted between the swallow tail sign disappearance score, bilateral maximum signal value of the locus coeruleus, bilateral melanin distribution volume of the substantia nigra, R2* value of the substantia nigra in the PD group, H-Y scale grading, and disease course duration. The results showed that the maximum signal value of the bilateral locus coeruleus was negatively correlated with disease course duration (right side: r=−0.345, P=0.029, left side: r=−0.380, P=0.016; *Figure 3A*). The smaller and average values of the bilateral locus coeruleus signal were negatively correlated with disease course duration (smaller: r=−0.334, P=0.035; average: r=−0.383, P=0.015; *Figure 3B*). The smaller volume of melanin in the bilateral substantia nigra was negatively correlated with H-Y scale grading (r=−0.325; P=0.041; *Figure 3C*), but there was no correlation between the average volume of melanin in the bilateral substantia nigra and disease course duration (r=−0.249; P=0.122) or H-Y scale grading (r=−0.285; P=0.075). In contrast, the disease course duration of patients with PD was positively correlated with H-Y scale grading (r=0.388; P=0.013; *Figure 3D*). However, swallow tail sign disappearance score did not show a significant correlation with H-Y scale grading (r=0.281; P=0.079) or disease course duration (r=−0.064; P=0.696). In addition, the correlation analysis between composite indicators and H-Y scale grading indicated that SWI and NM-MRI_SN_volume (r=−0.227; P=0.043); SWI and NM-MRI_LCmax (r=−0.239; P=0.032); SWI and T2*mapping_R2* (r=−0.268; P=0.029); SWI, NM-MRI_SN_volume, and NM-MRI_LCmax (r=−0.228; P=0.041); SWI, NM-MRI_SN_volume, and T2*mapping_R2* (r=−0.256; P=0.038); SWI, NM-MRI_LCmax, and T2*mapping_R2* (r=−0.301; P=0.014); and SWI, NM-MRI_SN_volume, NM-MRI_LCmax, and T2*mapping_R2* (r=−0.261; P=0.035) were negatively correlated with H-Y scale grading (*Figure 4A*). There was a negative correlation between PD disease course duration and NM-MRI_SN_volume and NM-MRI_LCmax (r=−0.247; P=0.027); NM-MRI_SN_volume and T2*mapping_R2* (r=−0.351; P=0.004); NM-MRI_LCmax and T2*mapping_R2* (r=−0.298; P=0.015); and NM-MRI_SN_volume, NM-MRI_LCmax, and T2*mapping_R2* (r=−0.346; P=0.005) (*Figure 4B*).

Diagnostic value of the combined MRI techniques

The diagnostic value of the disappearance of the SWI, NM-MRI_SN_volume, NM-MRI_LCmax, and T2*mapping_R2* was evaluated according to the clinical diagnosis of PD. The sensitivity, specificity, and AUC of a single index (*Figure 5A*, *Table 5*), 2 indices combined (*Figure 5B*, *Table 5*), and more than 2 indices combined (*Figure 5C*, *Table 5*) were analyzed. The results showed that the combination of all indices was the most effective in diagnosing PD. The Delong test comparison of single-index analysis, SWI (AUC =0.832), NM-MRI_SN_volume (AUC =0.889), and T2*mapping_R2* (AUC =0.777) showed no statistical difference in the diagnostic efficacy of PD (P>0.05), and the diagnostic efficacy each of the 3 indices was significantly higher than that of NM-MRI_LCmax (AUC =0.664) (P<0.05). In the analysis of combined multiple indices, it was found that SWI combined with NM-MRI_SN_volume could greatly improve the diagnostic efficacy of PD, and

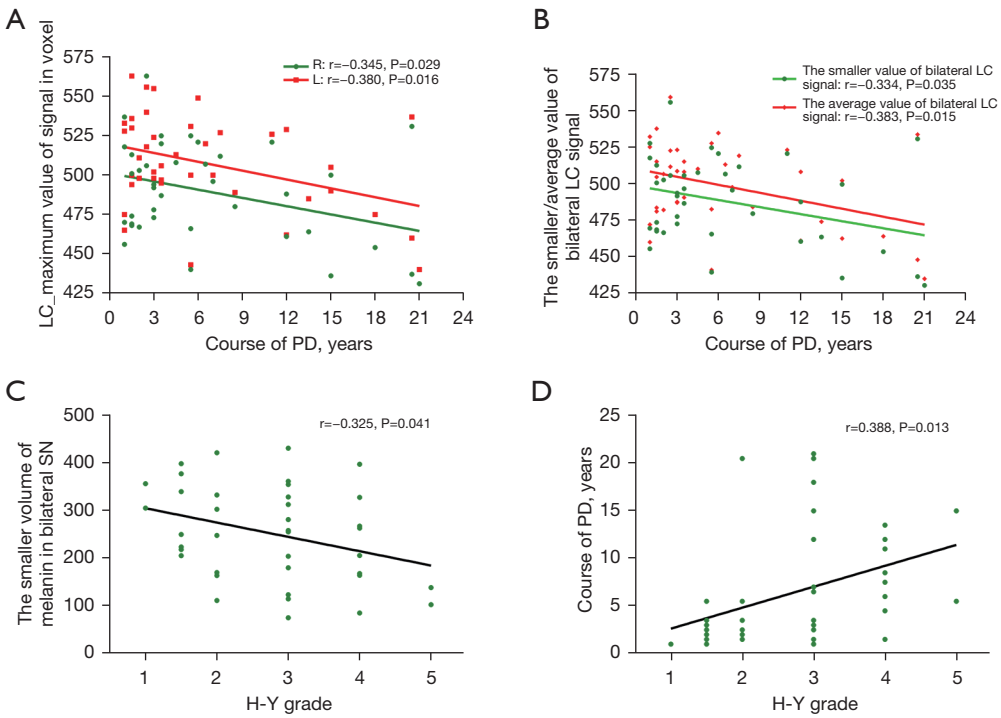

Figure 3 Correlation analysis of patients with PD. (A) Correlation analysis between the maximum value of bilateral locus coeruleus and the disease course duration of PD. (B) Correlation analysis between the smaller or average value of bilateral locus coeruleus signal and the disease course duration of PD. (C) Correlation analysis between the smaller distribution volume of melanin neurons in bilateral substantia nigra and H-Y grade. (D) Correlation analysis between the disease course duration of PD and H-Y grade in PD group. LC, locus coeruleus; R, right; L, left; PD, Parkinson disease; H-Y grade, Hoehn and Yahr grade; SN, substantia nigra.

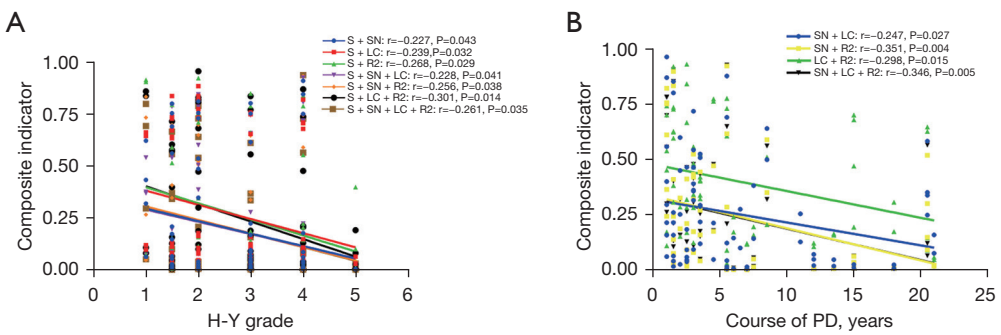

Figure 4 Correlation analysis of multitechnique indicators in patients with PD. (A) Some composite indicators were negatively correlated with H-Y scale grading, including S + SN, S + LC, S + R2, S + SN + LC, S + SN + R2, S + LC + R2, and S + SN + LC + R2. (B) Other composite indicators were negatively correlated with the disease course duration of PD, including SN + LC, SN + R2, LC + R2, and SN + LC + R2. S, swallow tail sign displayed on SWI; SN, distribution volume of NM-MRI melanin; LC, maximum signal value of locus coeruleus; R2, T2*mapping R2* value; SWI, susceptibility-weighted imaging; NM-MRI, neuromelanin-sensitive magnetic resonance imaging; PD, Parkinson disease.

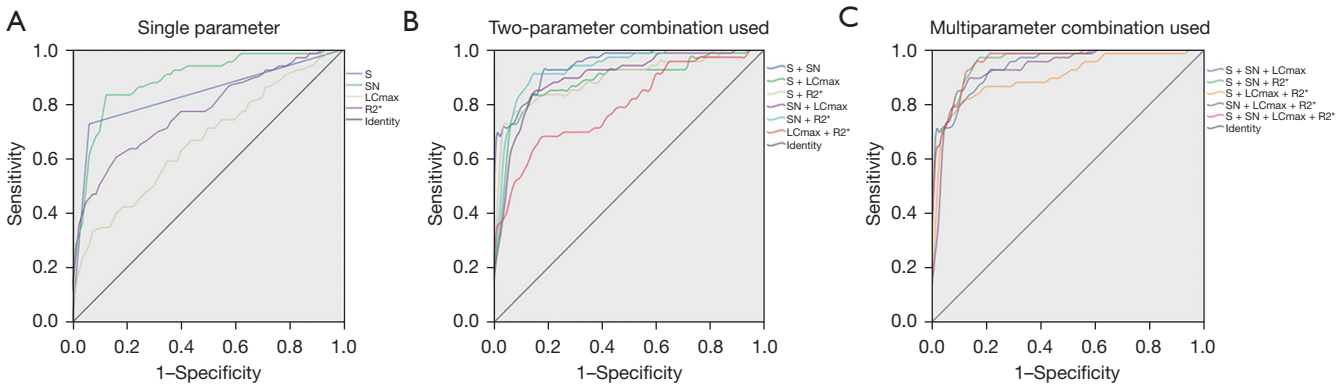

Figure 5 ROC curves of different sequence parameters in the PD group. (A) Single parameter for PD diagnosis. (B) Two-parameter combination used for PD diagnosis. (C) Multiparameter combination used for PD diagnosis. S, swallow-tail sign displayed on SWI; SN, distribution volume of NM-MRI melanin; LCmax, maximum signal value of locus coeruleus; R2*, T2*mapping R2* value; ROC, receiver operating characteristic; SWI, susceptibility-weighted imaging; NM-MRI, neuromelanin-sensitive magnetic resonance imaging; PD, Parkinson disease.

Table 5 Comparison of the diagnostic value of multiparameter MRI sequences

MRI sequence	AUC (95% CI)	Sensitivity	Specificity
SWI	0.832 (0.760, 0.905)	0.727	0.937
NM-MRI_SN_volume	0.889 (0.835, 0.944)	0.833	0.887
NM-MRI_LCmax	0.664 (0.575, 0.753)	0.667	0.562
T2*mapping_R2*	0.777 (0.700, 0.853)	0.606	0.837
SWI + NM-MRI_SN_volume	0.942 (0.907, 0.976)	0.924	0.825
SWI + NM-MRI_LCmax	0.880 (0.820, 0.940)	0.833	0.862
SWI + T2*mapping_R2*	0.890 (0.834, 0.946)	0.773	0.925
NM-MRI_SN_volume + LCmax	0.892 (0.839, 0.946)	0.848	0.850
NM-MRI_SN_volume + T2*mapping_R2*	0.929 (0.888, 0.971)	0.909	0.862
NM-MRI_LCmax + T2*mapping_R2*	0.791 (0.717, 0.865)	0.682	0.825
SWI + NM-MRI_SN_volume + LCmax	0.943 (0.909, 0.976)	0.924	0.800
SWI + NM-MRI_SN_volume + T2*mapping_R2*	0.958 (0.929, 0.986)	0.970	0.837
SWI + NM-MRI_LCmax + T2*mapping_R2*	0.899 (0.846, 0.953)	0.818	0.887
NM-MRI_SN_volume + LCmax + T2*mapping_R2*	0.931 (0.890, 0.972)	0.894	0.875
SWI + NM-MRI_SN_volume + LCmax + T2*mapping_R2*	0.958 (0.929, 0.986)	0.955	0.850

MRI, magnetic resonance imaging; AUC, area under the curve; CI, confidence interval; SWI, susceptibility-weighted imaging; NM-MRI, neuromelanin-sensitive magnetic resonance imaging; SN_volume, volume of melanin in the substantia nigra; LCmax, maximum value of the locus coeruleus signal.

there was no statistical difference in the diagnostic efficacy between the 2 indices in combination with other indexes (P>0.05). There was similarly no statistical difference between composite (2 or 3) indicators consisting of SWI and combinations consisting NM-MRI_SN_volume (P>0.05), but there were significant differences (P<0.05) between combined composite indicators with and without SWI and NM-MRI_SN_volume (P<0.05) (*Figure 6*).

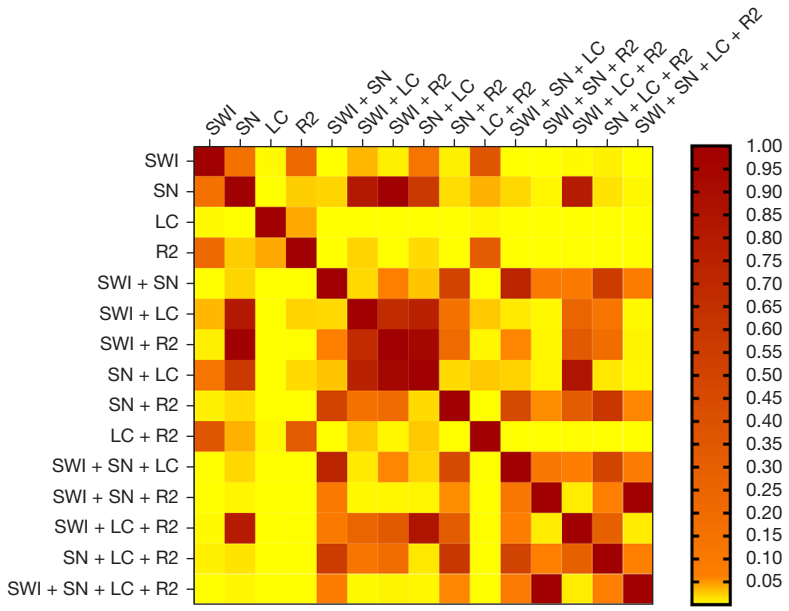

Figure 6 Delong test for the AUCs between different indicators. The color scale represents the magnitude of the P value of the AUC difference between different indicators in the Delong test. The critical values for yellow and orange are P=0.05, with P<0.05 showing a yellowish hue. SWI, susceptibility-weighted imaging; SN, distribution volume of NM-MRI melanin; LC, maximum signal value of the locus coeruleus; R2, T2*mapping R2* value; AUC, area under the curve; NM-MRI, neuromelanin-sensitive magnetic resonance imaging.

Discussion

This study focused on the analysis and comparison of SWI, NM-MRI, and T2*mapping sequences and their combination in diagnosing PD. The results showed that the swallow tail sign of the substantia nigra, the change of melanin neuron volume and the locus coeruleus signal in the substantia nigra, and the change of iron deposition in the substantia nigra had significant diagnostic value for PD; moreover, the combined use of multiple indices could significantly improve the diagnostic efficacy of PD compared with the use of single index. Our findings further demonstrated that improving the delineation method for the substantia nigra region and the measurement method for locus coeruleus signal intensity can improve the repeatability of analysis, which is helpful for the clinical detection and evaluation of individuals with PD.

Correlation analysis was conducted with clinical indicators to determine whether these indicators can detect PD earlier and evaluate the severity of the disease. The results suggested that the combined use of MRI parameters could diagnose and analyze PD from different angles and improve the diagnostic efficiency. The course and severity of PD can also be evaluated using certain indices or composite indicators.

Imaging sequences and their application value

SWI sequence detection of the bilateral swallow tail sign has high specificity, particularly for nigrosome 1. In this study, the disappearance of the swallow tail sign was detected in 2 cases in the right side and 3 cases in the left side of the control group. More disappearances were found in the PD group, which may be related to the pathogenesis of PD (15). The disappearance of the swallow tail sign in PD reflects the degeneration of dopamine neurons in the substantia nigra (16). Normally, nigrosome 1 has a high signal intensity on SWI. When nigrosome 1 neurons degenerate, the signal weakens or disappears, thus causing the disappearance of the swallow tail sign (15,16). In this study, the rate of disappearance of the swallow tail sign was significantly higher in the PD group than in the healthy control group. However, the disappearance of the swallow tail sign was not correlated with the disease course duration or H-Y grade, which is inconsistent with the previous studies (17-19). The lack of correlation in our study may be attributable to the relatively long disease course of the patients in the PD group and the limited number of cases.

This study was based on the delineation and volume measurement of melanin distribution in the substantia nigra. We found that the volume of melanin distribution

was significantly reduced in the PD group, reflecting a significant degeneration of melanin neurons (20,21). Sasaki *et al.* (22) used NM-MRI to simultaneously image the substantia nigra and locus coeruleus of patients with PD and healthy volunteers and compared the images with those of cadaveric specimens. The results showed that the areas of the substantia nigra and locus coeruleus with high signal intensity were significantly correlated with the distribution of melanin, and the signals of the corresponding areas of the substantia nigra and locus coeruleus of most patients with PD were weakened. In our study, the volume of melanin in bilateral substantia nigra of patients with PD was not correlated with disease course duration or H-Y grade, but a smaller volume of melanin in bilateral substantia nigra was negatively correlated with H-Y grade. The degeneration of melanin in the left and right sides of the substantia nigra might show individual differences, which is consistent with previously reported results indicating that the degree of melanin neuron degeneration was related to the severity of the disease (20,23,24).

Matsuura *et al.* (25) used NM-MRI to examine the substantia nigra area in terms of contrast-to-noise ratio and to follow-up patients with PD. They found that NM-MRI could be used to monitor disease progression. However, owing to the small sample size, the locus coeruleus could be accurately delineated and measured (10,26). The novelty of the present study is in the method analysis for measuring and obtaining the maximum signal strength value of the locus coeruleus tissue based on its high signal intensity. The results showed that the locus coeruleus signal in PD patients was significantly reduced. There was a statistical difference in the smaller value between the healthy control group and PD group. The smaller and average value of the bilateral locus coeruleus signal was negatively correlated with disease course. Therefore, the abnormal change of locus coeruleus signal may be useful for the early detection, evaluation, and monitoring of progression in patients with PD (27,28).

Bilateral substantia nigra signals showed no difference between the 2 groups examined in this study. This is likely due to the fact that the delineated area was taken as the average value of the signal calculated from the high signal intensity area while the signal attenuation area was not delineated. However, this also indirectly indicates that the high signal intensity in the sketched area was relatively accurate and did not contain many attenuation area signals, making the volume calculated in the sketched area more meaningful.

Compared with the SWI sequence, the T2*mapping sequence has advantages in quantitatively analyzing paramagnetic material (iron deposition) in the substantia nigra area. Considering that paramagnetic materials can shorten the T2 relaxation time, the T2* value in the corresponding area decreases while the R2* value increases (29,30). In this study, the PD group showed more significant changes in iron deposition than did the healthy control group, reflecting the correlation between the changes in iron deposition and the degeneration of PD neurons. However, the amount of iron deposition was not correlated with the H-Y grade or time of disease onset. This may indicate that indicators of neuron degeneration and disease course are not related to the amount of iron deposition in PD (31,32).

Diagnostic efficacy of multiple MRI techniques

Clinical diagnosis is often a comprehensive analysis of a disease from multiple perspectives, and in PD, using multiple sequences and multiple parameters may be necessary for validating the diagnosis. This study examined 4 image indicators measured through SWI, NM-MRI, and T2*mapping sequences to test the diagnostic efficacy of multiple sequences and multiple indices for PD. To this end, the sensitivity and specificity of the 4 imaging indicators and their combined use were analyzed, and the AUC values were compared. The higher the corresponding value was, the greater the clinical value of the corresponding image indicators for diagnosing PD. The results consistently point to shortcomings in the sensitivity and specificity of a single parameter. For example, SWI swallow tail sign had a higher specificity for diagnosing PD, but its sensitivity was not high, suggesting that it should be used in combination with other highly sensitive sequences, such as NM-MRI imaging indicators of the distribution volume of melanin in the substantia nigra. In this way, we can obtain higher sensitivity and specificity to improve the diagnostic efficacy of PD. In addition, we conducted a correlation analysis between the composite indicators used in combination with multiple indices and the disease course duration and H-Y grading: some composite indicators were negatively correlated with the H-Y grading, while others were negatively correlated with disease course duration. This indicates that the combination of multiple indices can not only improve the sensitivity and specificity of PD diagnosis but can also facilitate in the early clinical diagnosis and follow-up evaluation of patients with PD.

Study limitations

This study had some limitations. First, the sample size was not sufficiently large to compare the characteristic symptoms of PD with the image performance during the analysis of a certain characteristic symptoms of PD. In addition, the data of patients with the same high signal loss in the substantia nigra due to causes other than PD were not collected, nor were they compared with those of the PD group to ascertain their differences. The diagnostic interference analysis of NM-MRI based on the signal or volume change in different regions (e.g., cognition and motion) also requires further research (33,34). In the analysis of diagnostic efficacy, the sensitivity and specificity were not evaluated according to the disease stage (i.e., early and late PD), and thus additional data according to the disease stage should be collected. Moreover, there might have been empirical differences in physician evaluation of the swallow tail sign in the substantia nigra and in the delineation and measurement of the signal intensity in the substantia nigra. Given this, errors in the manual measurement of the image indicators might have occurred, but no further measurement or analysis of signal attenuation was conducted. Nevertheless, the evaluations were performed and agreed upon by 2 radiologists, and the average value of the measured indicators was used in the analysis to reduce the impact of errors.

Conclusions

The combination of multiple MRI techniques indicators, including the swallow tail sign in the substantia nigra, the distribution volume of melanin, the change of locus coeruleus signal, and R2* values based on T2*mapping can reflect the pathological mechanism of PD and disease course duration. Compared with use of a single indicator, the application of combined indicators is more beneficial for the diagnosis, treatment, and follow-up of patients with PD and has considerable value in clinical guidance. Inclusion of swallow tail sign in the substantia nigra and the distribution volume of melanin significant can significantly improve the diagnostic efficacy of composite indicators.

Acknowledgments

Funding: This study was supported by the Double New Projects of Health Science and Technology in Guangzhou (No. 20211A040003), the National Natural Science Foundation of China (No. 82171908), and the 2021 Yancheng Medical Science and Technology Development Project Grants-Yancheng Health Planning (2021) [No. 47(YK2021017)].

Footnote

Reporting Checklist: The authors have completed the STROBE reporting checklist. Available at https://qims.amegroups.com/article/view/10.21037/qims-23-87/rc

Conflicts of Interest: All authors have completed the ICMJE uniform disclosure form (available at https://qims.amegroups.com/article/view/10.21037/qims-23-87/coif). The authors have no conflicts of interest to declare.

Ethical Statement: The authors are accountable for all aspects of the work in ensuring that questions related to the accuracy or integrity of any part of the work are appropriately investigated and resolved. This study was approved by the ethics committee of Guangzhou Xinhai Hospital (No. GZXH-20200147) and was conducted according to the tenets of the Declaration of Helsinki (as revised in 2013). Written informed consent was obtained from all participants after detailed information concerning the research purpose, scanning duration, relevant risks, and examination considerations was provided.

References

1. Bloem BR, Okun MS, Klein C. Parkinson's disease. Lancet 2021;397:2284-303.
2. Dorsey ER, Constantinescu R, Thompson JP, Biglan KM, Holloway RG, Kieburtz K, Marshall FJ, Ravina BM, Schifitto G, Siderowf A, Tanner CM. Projected number of people with Parkinson disease in the most populous nations, 2005 through 2030. Neurology 2007;68:384-6.
3. Pyatigorskaya N, Sanz-Morère CB, Gaurav R, Biondetti

E, Valabregue R, Santin M, Yahia-Cherif L, Lehéricy S. Iron Imaging as a Diagnostic Tool for Parkinson's Disease: A Systematic Review and Meta-Analysis. Front Neurol 2020;11:366.
4. Trist BG, Hare DJ, Double KL. Oxidative stress in the aging substantia nigra and the etiology of Parkinson's disease. Aging Cell 2019;18:e13031.
5. Chen J, Cai T, Li Y, Chi J, Rong S, He C, Li X, Zhang P, Wang L, Zhang Y. Different iron deposition patterns in Parkinson's disease subtypes: a quantitative susceptibility mapping study. Quant Imaging Med Surg 2020;10:2168-76.
6. Wang Z, Luo XG, Gao C. Utility of susceptibility-weighted imaging in Parkinson's disease and atypical Parkinsonian disorders. Transl Neurodegener 2016;5:17.
7. Keil VC, Bakoeva SP, Jurcoane A, Doneva M, Amthor T, Koken P, Mädler B, Lüchters G, Block W, Wüllner U, Hattingen E. A pilot study of magnetic resonance fingerprinting in Parkinson's disease. NMR Biomed 2020;33:e4389.
8. Takahashi H, Watanabe Y, Tanaka H, Mihara M, Mochizuki H, Liu T, Wang Y, Tomiyama N. Quantifying changes in nigrosomes using quantitative susceptibility mapping and neuromelanin imaging for the diagnosis of early-stage Parkinson's disease. Br J Radiol 2018;91:20180037.
9. Kolpakwar S, Arora AJ, Pavan S, Kandadai RM, Alugolu R, Saradhi MV, Borgohain R. Volumetric analysis of subthalamic nucleus and red nucleus in patients of advanced Parkinson's disease using SWI sequences. Surg Neurol Int 2021;12:377.
10. Wang X, Zhang Y, Zhu C, Li G, Kang J, Chen F, Yang L. The diagnostic value of SNpc using NM-MRI in Parkinson's disease: meta-analysis. Neurol Sci 2019;40:2479-89.
11. Heim B, Krismer F, De Marzi R, Seppi K. Magnetic resonance imaging for the diagnosis of Parkinson's disease. J Neural Transm (Vienna) 2017;124:915-64.
12. Xing Y, Sapuan AH, Martín-Bastida A, Naidu S, Tench C, Evans J, Sare G, Schwarz ST, Al-Bachari S, Parkes LM, Kanavou S, Raw J, Silverdale M, Bajaj N, Pavese N, Burn D, Piccini P, Grosset DG, Auer DP. Neuromelanin-MRI to Quantify and Track Nigral Depigmentation in Parkinson's Disease: A Multicenter Longitudinal Study Using Template-Based Standardized Analysis. Mov Disord 2022;37:1028-39.
13. Fedeli MP, Contarino VE, Siggillino S, Samoylova N, Calloni S, Melazzini L, Conte G, Sacilotto G, Pezzoli G, Triulzi FM, Scola E. Iron deposition in Parkinsonisms: A Quantitative Susceptibility Mapping study in the deep grey matter. Eur J Radiol 2020;133:109394.
14. Ko SF, Yip HK, Zhen YY, Hung CC, Lee CC, Huang CC, Ng SH, Chen YL, Lin JW. Renal Damages in Deoxycorticosterone Acetate-Salt Hypertensive Rats: Assessment with Diffusion Tensor Imaging and T2-mapping. Mol Imaging Biol 2020;22:94-104.
15. Wang N, Liu XL, Li L, Zuo CT, Wang J, Wu PY, Zhang Y, Liu F, Li Y. Screening for Early-Stage Parkinson's Disease: Swallow Tail Sign on MRI Susceptibility Map-Weighted Images Compared With PET. J Magn Reson Imaging 2021;53:722-30.
16. Schneider E, Ng KM, Yeoh CS, Rumpel H, Fook-Chong S, Li HH, Tan EK, Chan LL. Susceptibility-weighted MRI of extrapyramidal brain structures in Parkinsonian disorders. Medicine (Baltimore) 2016;95:e3730.
17. Schwarz ST, Xing Y, Naidu S, Birchall J, Skelly R, Perkins A, Evans J, Sare G, Martin-Bastida A, Bajaj N, Gowland P, Piccini P, Auer DP. Protocol of a single group prospective observational study on the diagnostic value of 3T susceptibility weighted MRI of nigrosome-1 in patients with parkinsonian symptoms: the N3iPD study (nigrosomal iron imaging in Parkinson's disease). BMJ Open 2017;7:e016904.
18. Liu X, Wang N, Chen C, Wu PY, Piao S, Geng D, Li Y. Swallow tail sign on susceptibility map-weighted imaging (SMWI) for disease diagnosing and severity evaluating in parkinsonism. Acta Radiol 2021;62:234-42.
19. Lee TW, Chen CY, Chen K, Tso CW, Lin HH, Lai YL, Hsu FT, Chung HW, Liu HS. Evaluation of the Swallow-Tail Sign and Correlations of Neuromelanin Signal with Susceptibility and Relaxations. Tomography 2021;7:107-19.
20. Anderson DN, Charlebois CM, Smith EH, Arain AM, Davis TS, Rolston JD. Probabilistic comparison of gray and white matter coverage between depth and surface intracranial electrodes in epilepsy. Sci Rep 2021;11:24155.
21. Qian H, Kang X, Hu J, Zhang D, Liang Z, Meng F, Zhang X, Xue Y, Maimon R, Dowdy SF, Devaraj NK, Zhou Z, Mobley WC, Cleveland DW, Fu XD. Reversing a model of Parkinson's disease with in situ converted nigral neurons. Nature 2020;582:550-6.
22. Sasaki M, Shibata E, Tohyama K, Takahashi J, Otsuka K, Tsuchiya K, Takahashi S, Ehara S, Terayama Y, Sakai A. Neuromelanin magnetic resonance imaging of locus ceruleus and substantia nigra in Parkinson's disease. Neuroreport 2006;17:1215-8.
23. Sulzer D, Cassidy C, Horga G, Kang UJ, Fahn S, Casella L,

Pezzoli G, Langley J, Hu XP, Zucca FA, Isaias IU, Zecca L. Neuromelanin detection by magnetic resonance imaging (MRI) and its promise as a biomarker for Parkinson's disease. NPJ Parkinsons Dis 2018;4:11.
24. Reimão S, Pita Lobo P, Neutel D, Correia Guedes L, Coelho M, Rosa MM, Ferreira J, Abreu D, Gonçalves N, Morgado C, Nunes RG, Campos J, Ferreira JJ. Substantia nigra neuromelanin magnetic resonance imaging in de novo Parkinson's disease patients. Eur J Neurol 2015;22:540-6.
25. Matsuura K, Maeda M, Tabei KI, Umino M, Kajikawa H, Satoh M, Kida H, Tomimoto H. A longitudinal study of neuromelanin-sensitive magnetic resonance imaging in Parkinson's disease. Neurosci Lett 2016;633:112-7.
26. Giorgi FS, Lombardo F, Galgani A, Hlavata H, Della Latta D, Martini N, Pavese N, Ghicopulos I, Baldacci F, Coi A, Scalese M, Bastiani L, Keilberg P, De Marchi D, Fornai F, Bonuccelli U. Locus Coeruleus magnetic resonance imaging in cognitively intact elderly subjects. Brain Imaging Behav 2022;16:1077-87.
27. Zhou C, Guo T, Wu J, Wang L, Bai X, Gao T, Guan X, Gu L, Huang P, Xuan M, Gu Q, Xu X, Zhang B, Cheng W, Feng J, Zhang M. Locus Coeruleus Degeneration Correlated with Levodopa Resistance in Parkinson's Disease: A Retrospective Analysis. J Parkinsons Dis 2021;11:1631-40.
28. Prasuhn J, Prasuhn M, Fellbrich A, Strautz R, Lemmer F, Dreischmeier S, Kasten M, Münte TF, Hanssen H, Heldmann M, Brüggemann N. Association of Locus Coeruleus and Substantia Nigra Pathology With Cognitive and Motor Functions in Patients With Parkinson Disease. Neurology 2021;97:e1007-16.
29. Kan H, Uchida Y, Ueki Y, Arai N, Tsubokura S, Kunitomo H, Kasai H, Aoyama K, Matsukawa N, Shibamoto Y. R2* relaxometry analysis for mapping of white matter alteration in Parkinson's disease with mild cognitive impairment. Neuroimage Clin 2022;33:102938.
30. Du G, Lewis MM, Sica C, He L, Connor JR, Kong L, Mailman RB, Huang X. Distinct progression pattern of susceptibility MRI in the substantia nigra of Parkinson's patients. Mov Disord 2018;33:1423-31.
31. Ravanfar P, Loi SM, Syeda WT, Van Rheenen TE, Bush AI, Desmond P, Cropley VL, Lane DJR, Opazo CM, Moffat BA, Velakoulis D, Pantelis C. Systematic Review: Quantitative Susceptibility Mapping (QSM) of Brain Iron Profile in Neurodegenerative Diseases. Front Neurosci 2021;15:618435.
32. Cheng Q, Huang J, Liang J, Ma M, Zhao Q, Lei X, Shi C, Luo L. Evaluation of abnormal iron distribution in specific regions in the brains of patients with Parkinson's disease using quantitative susceptibility mapping and R2(*) mapping. Exp Ther Med 2020;19:3778-86.
33. Li QQ, Wu K, Xu JL, Yin L. White matter damage in patients with mild cognitive impairment in Parkinson's disease. Quant Imaging Med Surg 2022;12:1290-8.
34. Rong S, Li Y, Li B, Nie K, Zhang P, Cai T, Mei M, Wang L, Zhang Y. Meynert nucleus-related cortical thinning in Parkinson's disease with mild cognitive impairment. Quant Imaging Med Surg 2021;11:1554-66.

Cite this article as: Cao Q, Han X, Tang D, Qian H, Yan K, Shi X, Li Y, Zhang J. Diagnostic value of combined magnetic resonance imaging techniques in the evaluation of Parkinson disease. Quant Imaging Med Surg 2023;13(10):6503-6516. doi: 10.21037/qims-23-87

